SmartWater synergy with surfactant and polymer: A microscale investigation at crude oil-water interface

Subhash Ayirala[1*]*, Abdulkareem AlSofi*[1], Zuoli Li[2], Rubia Mariath[2], Zhenghe Xu[2], and *Ali Yousef*[1]

[1]EXPEC Advanced Research Centre, Saudi Aramco, Dhahran-31311, Saudi Arabia

[2] Department of Chemical and Materials Engineering, University of Alberta, Edmonton, Alberta T6G 1H9, Canada

Abstract. Different microscale interactions of surfactant, polymer, and surfactant-polymer with SmartWater, at crude oil/water interface, were studied by using interfacial shear rheometer, and Langmuir trough at both ambient and elevated temperatures. The reservoir crude oil is used and high salinity water (HSW) is selected as the base-line to provide representative comparisons SmartWater. An amphoteric surfactant (1,000 ppm) and sulfonated polyacrylamide polymer (500 ppm) are chosen for this experimental investigation. Interfacial shear rheology results showed that viscoelasticity of interface is reduced with SmartWater in comparison to HSW. Such decrease in viscoelasticity is quite evident with the reductions observed in both viscous and elastic modulus data. Polymer either alone or together with surfactant resulted in relatively lower elasticity for SmartWater when compared to HSW. Interfacial pressures with polymer remained almost the same as brines, however they decreased with SmartWater. Surfactant significantly reduced the interface pressures and these reductions in interface pressures were greater with SmartWater when compared to HSW. The interface compression energies were reduced by approximately two orders of magnitude with surfactant. SmartWater also showed better efficacy to lower the interface compression energies over HSW in the presence of surfactant. These consistent findings obtained from interface viscoelasticity, interface pressures and compression energies demonstrated the favorable microscale interactions of surfactant and polymer chemicals with SmartWater to result in the formation of less rigid films at crude oil-water interface. Such softer interfacial films can easily be destabilized to improve oil phase connectivity and mobilize incremental oil in chemical enhanced oil recovery (EOR) processes.

1 Introduction

In the past few years, the potential synergy between SmartWater flooding and chemical Enhanced Oil Recovery (EOR) has attracted significant attention. Several laboratory studies have demonstrated the potential value of combining the two EOR methods. Early studies focused on the potential synergy between SmartWater and polymer flooding (Ayirala et al., 2010; Torrijos et al., 2018; AlSofi et al., 2018; AlSofi et al., 2019). Later studies focused on SmartWater or low-salinity water synergy with surfactant and surfactant-polymer flooding (Wang et al., 2018; Ayirala et al., 2019; Moradi et al., 2019; Eslahati et al., 2020; Veiskarami et al., 2020; Al-Murayri et al., 2021).

All these reported studies focused on macroscopic scale observations and relied heavily on macroscopic experiments. Displacement experiments – core imbibition in Eslahati et al. (2020), and corefloods in most of the remaining – formed the major component of previous studies. Such displacement results were complemented by measurements such as polymer rheology (Ayirala et al., 2010; AlSofi et al., 2019), surface-potential (AlSofi et al., 2019; Ayirala et al., 2019), interfacial tension (AlSofi et al., 2019; Ayirala et al., 2019; Moradi et al., 2019; Eslahati et al., 2020), contact angle (AlSofi et al., 2019; Ayirala et al., 2019; Moradi et al., 2019; Eslahati et al., 2020; Veiskarami et al., 2020), and phase behavior (Ayirala et al., 2019; Veiskarami et al., 2020; Al-Murayri et al., 2021). Also these studies have attempted to explain the underlying microscopic mechanisms of the observed synergism through the results obtained from macroscopic to core scale experiments. For example, AlSofi et al. (2018) noted that many of the observed effects of SmartWater on polymer injectivity and transport can be attributed to polymer coil expansion in the lower-salinity SmartWater.

So clearly, besides some limited hypothetical attempts, little attention has been given to uncovering the underlying synergistic micro-scale mechanisms in play. Therefore, in this work, we study the potential synergies between SmartWater and chemical EOR (surfactant, polymer, and surfactant-polymer) at the microscale. The study scope includes a thorough primary suite of interfacial measurements (interfacial shear rheometry and Langmuir trough) together with a complementary comprehensive characterization of fluids (both brines and chemical solutions). These interfacial experiments characterize crude oil/water interfaces – obtained with the different brines and chemical solutions – in terms of interface viscoelasticity, interface pressure, and interface compression energies. The main objectives of this study are: (1) use the interfacial results to uncover some of the potential micro-scale synergies between SmartWater and chemical EOR, and (2) discuss the applicability of these findings in terms of macro-scale implications and more specifically oil mobilization.

2 Experimental Materials and Methods

2.1 Materials

Brines: different salts such as magnesium chloride, calcium chloride dehydrate, anhydrous sodium sulfate, sodium chloride, and sodium bicarbonate were used to prepare two different synthetic-brine solutions using the deionized (DI) water. These salt compounds are obtained from Fisher Scientific, and all were American Chemical Society (ACS) grade certified. The thermos Scientific NanoPure™ system was used to produce DI water with a resistivity of 18.2

---

* Corresponding author: nethajisubhash.ayirala@aramco.com

MΩ·cm at 25°C. The salinity of two different synthetic brines used in experiments are shown in Table 1.

Table 1. Synthetic brine compositions used.

Ions	High Salinity Water (HSW) (ppm)	SmartWater (SW) (ppm)
Na^+	18,300	1,824
Ca^{2+}	650	65
Mg^{2+}	2,110	211
SO_4^{2-}	4,290	429
Cl^-	32,200	3,220
HCO_3^-	120	12
TDS	57,670	5,761

Chemicals: A high molecular weight sulfonated polyacrylamide polymer is used. This polymer (P) had a molecular weight of 12 million Dalton with a sulfonation degree of 25 mol%. The surfactant used is amphoteric, which is betaine-type with an active content of 50%. Both these surfactant (S) and polymer (P) chemicals are chosen, since they were reported to be tolerant to high salinity and high temperature conditions (Han et al., 2014; Jouenne, 2020; Wang et al., 2015).

Water conditions: amphoteric surfactant, and/or sulfonated polyacrylamide polymer were added to HSW and SW brines, respectively to prepare the polymer in brine, surfactant in brine, and polymer plus surfactant in brine solutions. Together with the baseline of HSW and SW, all the water conditions tested in the current study are listed in Table 2.

Table 2. Different water conditions used in experiments.

Base case runs (2)	HSW, SW
Surfactant runs (2)	HSW+1000 ppm S SW+1000 ppm S
Polymer runs (2)	HSW+500 ppm P SW+ 500 ppm P
Surfactant-polymer runs (2)	HSW+1000 ppm S + 500 ppm P SW+ 1000 ppm S + 500 ppm P

2.2 Viscosity of polymer solutions

The viscosities of polymer in brine solutions were measured with a rheometer (AR-G2 Rheometer, TA Instruments) supported by TRIOS software (TA Instruments), using the 60 mm plate method with shear rate increasing from 1 s^{-1} to 100 s^{-1}. Rheometer was well calibrated before using it for viscosity measurements. Freshly prepared polymers solutions were kept at room temperature and used within 12 hours after preparation. A thermostat water bath was used to keep temperature constant at either 23°C or 70°C during the measurements.

2.3 Geochemical analysis of crude oil

SARA analysis. SARA analysis was done with crude oil samples to determine the fraction amount of saturates, aromatics, resins and asphaltenes in the sample by following the ASTM D2007-03 test procedure. The test, designed depending on the polarizability and polarity of each fraction, took about 8 days. Asphaltenes are not soluble in heptane and can be precipitated out from the crude oil by adding heptane. Aromatics were adsorbed with silica gel and resins were adsorbed with clays. Saturates cannot be adsorbed by these solids and were flushed off the column with heptane.

Total acid number (TAN) and Total base number (TBN). The TAN measurement followed ASTM D664 protocol, while TBN measurement is done using ASTM D4739 protocol. Both analyses were done by Maxxam Analytics Edmonton.

Density and viscosity. The viscosity of crude oil was measured with a digital density meter (Model DDM 2910, Rudolph Research Analytical). Crude oil was introduced into the cell and kept inside for 5 minutes to stabilize at 23°C and 70°C, respectively. Viscosity values were read after stabilization and the density values were given by the density meter based on the viscosity values.

2.4 Shear rheology

The viscoelastic properties (G', elastic and G", viscous) of the crude oil-water (different brine compositions, surfactant and/or polymer) interfacial layers were determined using an AR-G2 stress-controlled rheometer (TA Instruments, New Castle, DE, USA) equipped with a double-wall ring (DWR) geometry, which is made of Pt/Ir. The radius of the DWR is 35 mm and its square-edged cross section helps to pin it on the water-oil interface, as shown in Figure 1a. The ring was flamed before each experiment to remove all the organic contaminants. A Delrin trough with a circular channel as the sample holder was attached to a Peltier plate for temperature control, as shown in Figure 1b.
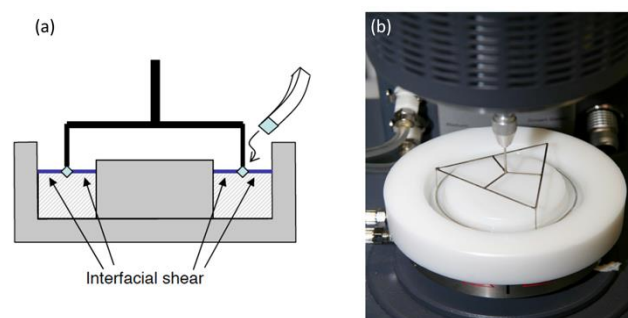

Fig. 1. (a) Illustration of the DWR configuration, and (b) the setup on the AR-G2 rheometer.

Pipetted into the sample holder was firstly 19.2 mL aqueous solution as the bottom phase or sub-phase. After positioning the ring at the air-aqueous solution interface, 15 mL of crude oil was slowly pipetted onto the top of the aqueous phase. Finally, a Teflon cap was placed over the sample to prevent solvent evaporation. To study the effect of aging on viscoelastic properties of interfacial layers, time sweeps were conducted at an angular frequency of 0.3 Hz and

with a 0.8% strain amplitude for 7 hrs. The measurements were conducted at 70 ± 0.1°C.

2.5 Langmuir trough

The compressional behavior of interfacial films at the dectol/water (different brine compositions, surfactant and/or polymer) interface was characterized by interfacial pressure-area (π-A) isotherm obtained through a Langmuir trough. The experiments were conducted using a computer-controlled KSV trough (Biolin Scientific, Espoo, Finland) whose area is 250 cm². A paper Wilhelmy plate sensor (Biolin Scientific; product identification, KN 0005) was used to detect the interfacial pressure (π) which represents the change in the interfacial tension (IFT) due to the presence of interfacial material relative to the clean interface (IFT_0), and is given by

$$\pi = IFT_0 - IFT \qquad (1)$$

Prior to each measurement the trough was carefully cleaned with toluene, acetone, and Milli-Q water respectively. As shown in Figure 2, the lower part of the trough was filled with 120 mL of Milli-Q water solutions as the subphase. The trough was considered clean when the pressure isotherm at the air-DI water interface has a pressure reading of within ±0.1 mN/m with the water phase being compressed from 250 cm² to 25 cm². The barriers were then fully expanded, and the balance was zeroed at clean air-water interface. 100 mL of dectol (volume of decane: toluene=50:50) was then added to the top of DI water as the top phase. 23 μL of 20 wt% crude oil in toluene solution was then injected into top dectol phase using a Hamilton gastight syringe. After equilibrating the film for 1 hour, the system was compressed at 10 mm/min to obtain the isotherms. DI water was replaced by brine solutions with/without polymer and/or surfactants to study the effect of polymer and surfactants on the compressional behavior of oil/water interface.
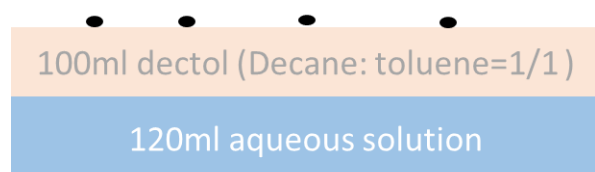

Fig. 2. Illustration showing the addition of water and oil phases in the trough for Langmuir trough measurements.

3 Results and Discussion

3.1 Characterization of brine solutions and crude oil

Brine/polymer solutions. The viscosity of both brine and polymer solutions measured as a function of temperature at 23°C and 70°C are shown in Figure 3 (a) and 3 (b), respectively. As shown in the Figure, the viscosity of polymer solutions decreases with increasing shear rate at both the temperatures while the viscosity of brines is almost constant at different shear rates, indicating that the polymer solutions are non-Newtonian and shear-thinning. The viscosity of all brine and polymer solutions is higher at 23°C than at 70°C.

As expected, higher viscosities were obtained with polymer in SmartWater (SW) at different shear rates in comparison to high salinity water (HSW) at the same temperature. Such result is obvious by considering the well-established favorable effect of lower salinities on viscosifying characteristics of polyacrylamide and sulfonated polyacrylamide polymers (Ayirala et al., 2010; AlSofi et al., 2019). The measured viscosities of HSW, SW, HSW + 500 ppm polymer, and SW + 500 ppm polymer at 6.3 sec⁻¹ shear rate and 23°C were found to be 1.0 cP, 0.93 cP, 3.6 cP, and 4.9 cP, respectively. Similarly, the viscosities of these respective solutions at 6.3 sec⁻¹ shear rate and 70°C were measured as 0.70 cP, 0.49 cP, 3.2 cP, and 4.2 cP.
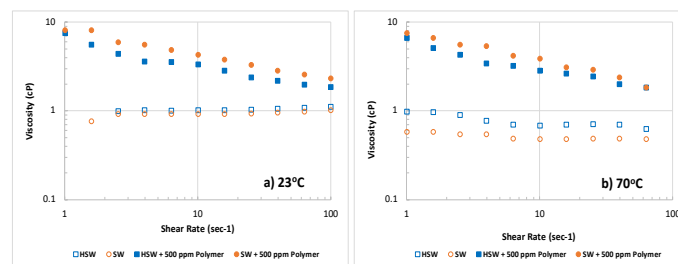

Fig. 2. Viscosity of brine/polymer solutions as function of shear rate at 23°C (a) and 70°C (b).

Crude oil. Total acid number (TAN) and total base number (TBN) of crude oil analyzed by Maxxam Analytics Edmonton are shown in Table 3. As can be seen, the oil is relatively acidic in nature due to the presence of predominantly acidic fractions over basic components.

Table 2. TAN and TBN of crude oil.

Analysis	Crude oil
TAN (mg KOH/g)	0.47
TBN (mg KOH/g)	0.04

Based on the SARA analysis, the crude oil had a much lower content of asphaltenes, while the contents of saturates, aromatics and resins are found to be higher in comparison to asphaltenes (Table 4).

Table 3. SARA analysis results (in wt%) for crude oil.

Parameter	Crude oil
Saturates	50.67%
Aromatics	17.12%
Resins	20.94%
Asphaltenes	1.65%

As can be seen from Table 5, the viscosity of crude oil was lowered significantly as the temperature was increased from room temperature to 70°C. The decreasing of density upon increasing temperature was also quite evident. At room temperature, the viscosity of crude oil was measured to be about 19.2 cP, while the viscosity decreased to 2.3 cP at 70°C.

Table 4. Density and viscosity of crude oil.

Property	Crude oil (23°C)	Crude oil (70°C)
Density (gm/cc)	0.87	0.84
Viscosity (cP)	19.2	2.3

3.2 Interface viscoelasticity

The elastic (G') and viscous (G") modulus for crude oil/brine interface obtained with HSW and SW at 70°C are shown in Figure 4. As shown in this figure, the crude oil/brine interface was elastic-dominant (G'>G") from the beginning, and there was no significant increase in moduli of the oil/brine interface even after aging for 7 hours. Such buildup of elasticity for oil-water interface may be caused by the accumulation of asphaltenes at the interface to form a rigid network of asphaltenic structures (Freer et al., 2003). At high temperatures, it is expected that asphaltene molecules would move faster and quickly accumulate at the interface to result in early elastic dominant behavior. Interestingly, the elastic modulus of interface was found to be higher with HSW when compared to SW. But only minor increase in viscous modulus was observed with HSW. The interface viscoelasticity is primarily governed by the competitive adsorption between asphaltene and the non-asphaltenic components of crude oil, such as naphthenic acids (Yarranton et al., 2007; Moradi et al., 2013; Alves et al., 2014). The adsorption of surface-active components at the interface is dominated by asphaltenes when compared to naphthenic acids in HSW (Verruto et al. 2009; Moradi et al. 2013). The asphaltenes adsorb onto the interface, while naphthenic acids remain in the bulk aqueous phase at this high salinity thereby resulting in the formation of a rigid viscoelastic film.
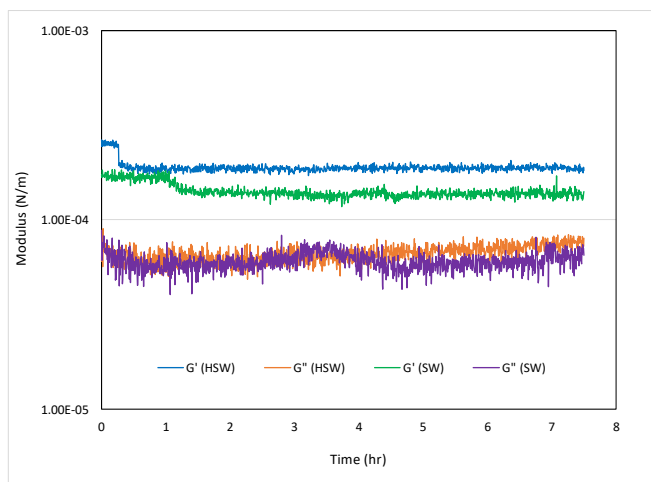

Fig. 4. Viscous and elastic moduli of interface with HSW and SW brine solutions at 70°C.

The viscoelasticity data of the oil/water interface obtained with 1,000 ppm surfactant in both HSW and SW brines at 70°C are presented in Figure 5. As can be seen, surfactant decreased the elastic modulus in HSW but increased the elasticity in SW. However, the addition of surfactant showed no effect on viscous modulus in both HSW and SW brines. The measured viscous and elastic modulus data obtained at crude oil/water interface with HSW+polymer and SW+polymer solutions at 70°C are shown in Figure 6. These results confirmed the impact of polymer on elastic modulus, wherein the elasticity of the interface has been found to be higher with HSW in the presence of polymer. This behavior is contrastingly opposite to that observed with HSW + surfactant solution. However, the viscous modulus almost remained the same for both HSW+polymer and SW+polymer solutions. Figure 7 summarizes the viscous and elastic modulus results obtained with surfactant + polymer in HSW

and SW brines at 70°C. From these results, it is quite evident that both elastic and viscous modulus are higher with HSW in the presence of surfactant + polymer. Such finding intuitively suggests that interface viscoelasticity is mainly dictated by polymer rather than surfactant when both the chemicals are present. This may be due to increased viscosities of aqueous phase caused by polymer, which forms a viscous barrier that would either slow down or prevent the movement of surfactant molecules to the interface.
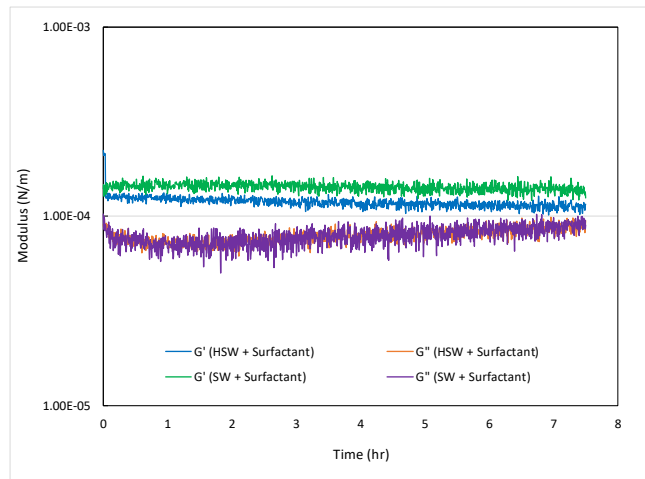

Fig. 5. Viscous and elastic moduli of interface with HSW+surfactant and SW+surfactant solutions at 70°C.
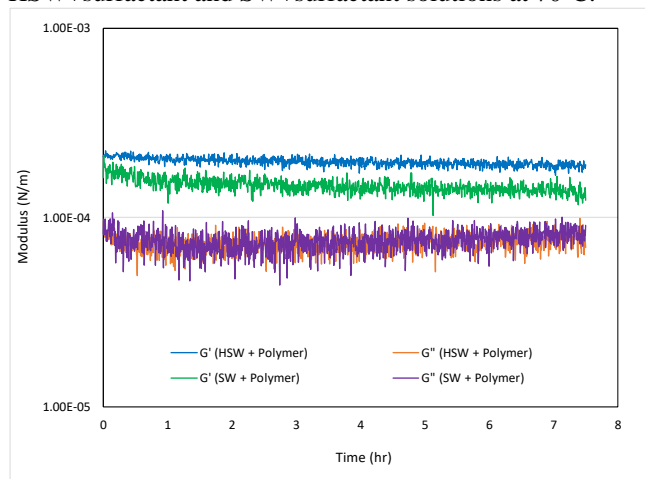

Fig. 6. Viscous and elastic moduli of interface with HSW+polymer and SW+polymer solutions at 70°C.
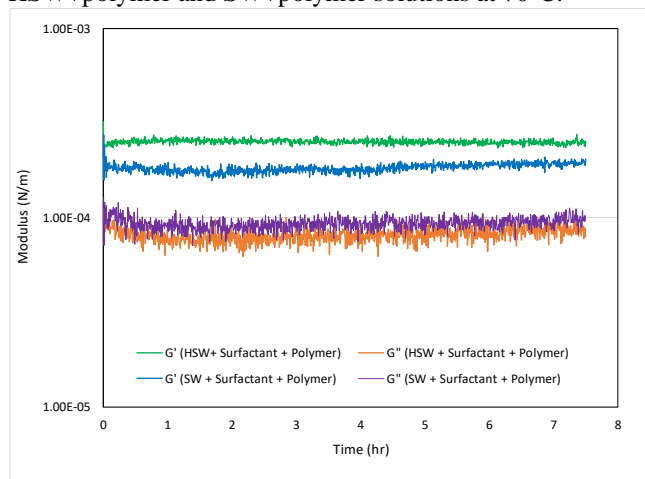
Fig. 7. Viscous and elastic moduli of interface with HSW+surfactant+polymer and SW+surfactant+polymer solutions at 70°C.

Overall, the results described in this section demonstrated the beneficial synergy of SmartWater on interface viscoelasticity either alone or in combination with polymer and surfactant + polymer. The lower salinity of SmartWater can decrease the elasticity of interfacial film to make it less rigid. These less rigid oil-water interfacial films can quickly be destabilized to promote the coalescence between oil droplets. Such faster coalescence of oil droplets would eventually improve oil phase connectivity for easy mobilization of oil in chemical EOR processes.

3.3 Interfacial pressures and compression energies

The effect of brine composition on the interfacial pressure was studied by recording the oil-water interfacial pressure (π) as the oil-brines/DI water interface area was compressed (A) at ambient temperature (23°C). Figure 8 presents the interfacial pressure vs. area isotherms obtained with brine and brine + polymer solutions. As illustrated in Figure 8, the interfacial pressure increases with the compressing of the surface area. Because the compressional viscoelastic moduli are proportional to the ratio between the changes in interfacial pressure and in the compressed area, the slope of the π–A isotherms is an indication of the rigidness of the interfacial layer and steeper isotherms represent more rigid oil-aqueous phase interfacial layers. Obviously, the interfacial film was most rigid in brines, and became less rigid with the addition of polymer. The interfacial pressures are highest with HSW followed by SW, HSW+polymer, and SW+polymer, respectively. These results indicated that rigidity of oil-water interfacial film is decreased by SmartWater and the lowest interfacial pressures obtained with SW+polymer also demonstrate the favorable synergy of SmartWater with polymer to form less rigid films at oil-water interface.
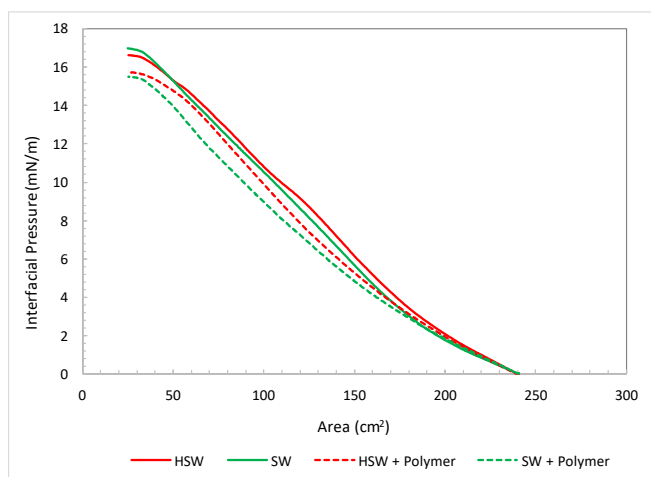

Fig. 8. Effect of brine compositions and polymer on π-A isotherms obtained for interfacial films at the diluted crude oil-brine interfaces at 23°C.

The interfacial pressure vs. area isotherms obtained by the addition of surfactant at different concentrations to HSW and SW brines at 23°C are shown in Figure 9. As can be seen, the interfacial pressures are significantly reduced by the addition of surfactant to both HSW and SW brines. The high efficiency of surfactant in softening the interfacial film was confirmed even at lower surfactant concentrations of 125 ppm and 10 ppm. It is interesting to note that the interfacial pressure was decreased to lower than 1 mN/m at a much lower surfactant concentration of 10 ppm. Almost two orders of magnitude reduction in interfacial pressure was observed at 1000 ppm surfactant concentration to result in interfacial pressure values lower than 0.1 mN/m. Another important point to be highlighted is that interfacial pressures obtained with SW brine at each surfactant concentration is relatively lower than that obtained with HSW brine. This observation confirms the synergistic effect of SW brine with surfactant to result in lower interfacial pressures and subsequently decrease the rigidity of oil-water interfacial film.
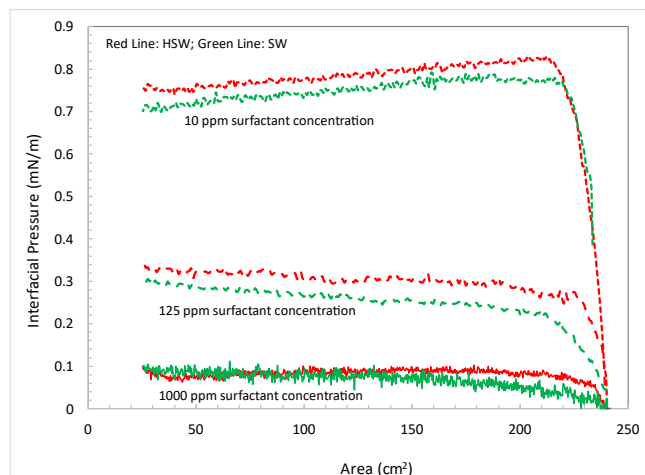

Fig. 9. Effect of surfactant on π-A isotherms obtained for interfacial films at the diluted crude oil-brine interfaces at 23°C.

Figure 10 presents the interface pressure vs. area isotherms obtained with surfactant + polymer in HSW and SW brines at 23°C. Since both of polymer and surfactant can soften the film, it is reasonable to see the lowest interfacial pressure in the brine solution with both of surfactant and polymer due to their combined effect. Similar to those results observed with either polymer or surfactant, SmartWater showed lower interfacial pressures with surfactant + polymer to confirm the favorable synergy even when both the chemicals are present together in the aqueous solution.
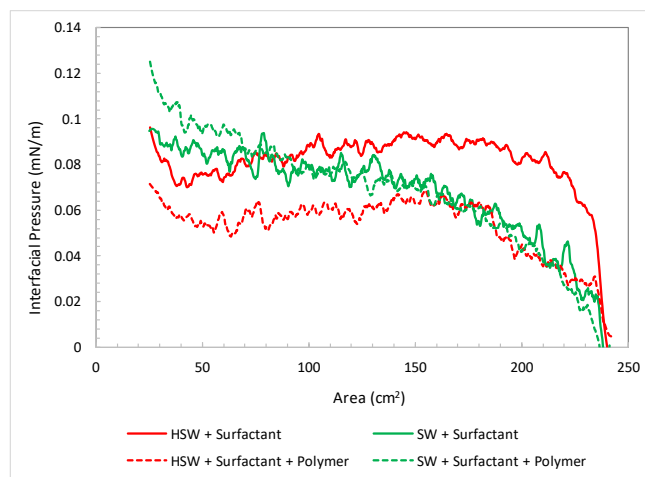
Fig. 10. Effect of surfactant-polymer on π-A isotherms obtained for interfacial films at the diluted crude oil-brine interfaces at 23°C.

The compression energy, calculated by the integration of interfacial pressure from π-A isotherms over the surface area, directly quantifies the film rigidity as it represents the difficulty to compress the interface. As shown in Figure 11, while the compression energy is comparable in HSW and SW brines, it is decreased by the addition of polymer or surfactant, and is lowest with the combination of surfactant and polymer. Surfactant by itself is found to be very effective to soften the interfacial film by significantly lowering the interfacial compression energy by almost two orders of magnitude. SmartWater brine lowered the interface compression energy at all conditions including the brine, brine + polymer, brine + surfactant, brine + surfactant + polymer when compared to the HSW brine. These results showed consistent trends with viscoelasticity and interfacial pressure data discussed earlier to demonstrate very well that SmartWater can synergistically combine with the beneficial effects of surfactant, polymer, surfactant-polymer to result in favorable microscale interactions at oil-water interface. Such favorable interactions can develop less rigid oil-water interfaces, which can easily be destabilized to fasten the coalescence between oil droplets to form larger oil ganglia and quickly form oil bank in chemical EOR processes.
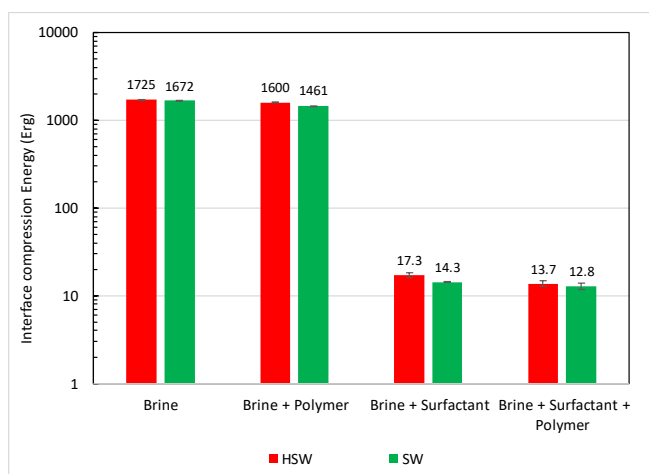

Fig. 11. Compression energy for the diluted crude oil-brines/DI water interface with brine, brine + polymer, brine + surfactant, and brine + surfactant + polymer solutions at 23°C.

3.4 Relationship between interfacial film rigidity and oil mobilization

In surfactant based tertiary chemical EOR processes, the residual oil droplets trapped in pore throats are released by the reductions in capillary forces caused by lowering of oil-water interfacial tension (IFT) at fluid-fluid interface and favorable wettability alteration at rock-fluids interface. The released oil droplets should reconnect with each other to grow into larger oil ganglia and sequential coalescence of these larger ganglia eventually forms a small oil bank. This small oil bank once formed grows bigger and bigger in size as it effectively reconnects additional ganglia in the flow path. The reconnection of oil ganglia mainly occurs through coalescence of oil droplets. The coalescence process happens when the interfacial film between the two oil droplets is

drained to eventually become very thin and rupture, which is directly linked with the rigidity of the interfacial film. As the interfacial film is less rigid, it can be ruptured at a higher critical film thickness to commence the coalescence process and fasten the time required to complete the coalescence between oil droplets.

Even though oil-releasing from rock surface is critical to chemical EOR process, by sole means it is not sufficient to result in efficient oil mobilization. It is most likely possible that without the coalescence of oil droplets after their release from the rock, the droplets will largely remain isolated in the production path. Such isolation can result in further breakup and re-entrapment of oil droplets in pore throats to adversely impact the recovery efficiency. Relatively lower interface viscoelasticities, interfacial pressures, and compression energies observed with SmartWater in comparison to HSW with surfactant, polymer, and surfactant-polymer chemicals indicate the ability of SmartWater to lower the oil-water interfacial film rigidity in chemical EOR. As a result, the use of SmartWater as injection fluid in chemical EOR processes can quickly destabilize the oil-water interfacial film to promote the coalescence between oil droplets and improve the connectivity of oil phase for easy oil mobilization (Figure 12). These favorable effects hasten the formation of oil bank not only to accelerate oil production but also to increase oil recovery in chemical EOR.
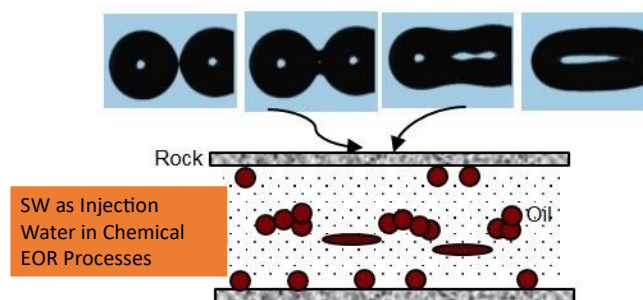

Fig. 12. Schematic representing the enhanced coalescence between oil droplets for improved oil phase connectivity in chemical EOR with SW as injection water.

4 Conclusions

In this experimental investigation, we presented the results obtained from interfacial shear rheology and Langmuir trough measurements to explore the micro-scale synergistic effects of SmartWater with surfactant, polymer, and surfactant-polymer chemicals at crude oil-water interface. The experimental data analyzed include interface viscous and elastic modulus (viscoelasticity), interface pressures and compression energies. The data showed consistent trends to demonstrate the favorable effects of SmartWater to lower the rigidity of oil-water interfacial film in the presence of surfactant, polymer, surfactant-polymer. These favorable effects can promote the coalescence of oil droplets to improve oil phase connectivity and oil mobilization in chemical EOR. The main conclusions are summarized in the following:

- SmartWater reduced both viscous and elastic modulus of the interface when compared to HSW. There was no impact of SmartWater on viscous modulus with surfactant, polymer, and surfactant-polymer. However, the elasticity of interface is lowered by SmartWater in combination with polymer and surfactant-polymer.
- Interfacial pressures were lowered by SmartWater, over HSW, at all water conditions including brine, brine-polymer, brine-surfactant, and brine-surfactant-polymer. Both polymer and surfactant are effective in lowering the interfacial pressure, while surfactant showed the highest efficiency to reduce interfacial pressures by almost two orders of magnitude.
- Interfacial compression energies also confirmed the favorable effect of SmartWater to effectively synergize with surfactant, polymer, surfactant-polymer to increase the easiness to compress the interface. The lowest interface compression energies are obtained with SmartWater in the presence of surfactant and surfactant-polymer.
- These results on viscoelasticity, interfacial pressure, and compression energies agreed very well with each other to demonstrate that SmartWater can synergistically combine with the beneficial effects of surfactant, polymer, surfactant-polymer to result in favorable microscale interactions at oil-water interface.
- Such favorable interactions can develop less rigid oil-water interfaces, which can easily be destabilized to fasten the coalescence between oil droplets to form larger oil ganglia and quickly form oil bank in chemical EOR processes.

References

Al-Murayri, M.T., Kamal, D.S., Al-Qattan, A., Winoto, W., Li, Z., Britton, C. and Delshad, M., 2021. A practical and economically feasible surfactant EOR strategy: Impact of injection water ions on surfactant utilization. Journal of Petroleum Science and Engineering 201:108479.

AlSofi, A.M., Wang, J. and Kaidar, Z.F., 2018. SmartWater synergy with chemical EOR: Effects on polymer injectivity, retention and acceleration. Journal of Petroleum Science and Engineering 166: 274-282.

AlSofi, A.M., Wang, J., AlBoqmi, A.M., AlOtaibi, M.B., Ayirala, S.C. and AlYousef, A.A., 2019. Smartwater synergy with chemical enhanced oil recovery: Polymer effects on smartwater. SPE Reservoir Evaluation & Engineering 22 (01): 61-77.

Alves, D.R., Carneiro, J.S.A., Oliveira, I.F., Façanha, F., Santos, A.F., Dariva, C., Franceschi, E. and Fortuny, M. 2014. Influence of the salinity on the interfacial properties of a Brazilian crude oil–brine systems, Fuel 118: 21-26.

Ayirala, S.C., Uehara-Nagamine, E., Matzakos, A., Chin, R., Doe, P. and van Den Hoek, P. A designer water process for offshore low salinity and polymer flooding applications. 2010. SPE-129926-MS. SPE Improved Oil Recovery Symposium, Tulsa, Oklahoma, USA.

Ayirala, S.C., Boqmi, A., Alghamdi, A., and AlSofi, A.M. 2019. Dilute surfactants for wettability alteration and enhanced oil recovery. Journal of Molecular Liquids 285: 707-715.

Eslahati, M., Mehrabianfar, P., Isari, A.A., Bahraminejad, H., Manshad, A.K. and Keshavarz, A., 2020. Experimental investigation of Alfalfa natural surfactant and synergistic effects of Ca^{2+}, Mg^{2+}, and SO_4^{2-} ions for EOR applications: interfacial tension optimization, wettability alteration and imbibition studies. Journal of Molecular Liquids 310: 113123.

Freer, E.M., T. Svitova, T. and Radke, C.J. 2003. The role of interfacial rheology in reservoir mixed wettability, Journal of Petroleum Science and Engineering 39: 137-158.

Han, M., Fuseni, A., Zahrani, B. and Wang, J. 2014. Laboratory study on polymers for chemical flooding in carbonate reservoirs. SPE-169724-MS. SPE EOR Conference at Oil and Gas West Asia. Muscat, Oman.

Jouenne, S. 2020. Polymer flooding in high temperature, high salinity conditions: selection of polymer type and polymer chemistry, thermal stability. Journal of Petroleum Science and Engineering 195: 107545.

Moradi, M., Topchiy, E., Lehmann, T.E. and Alvarado, V. 2013. Impact of ionic strength on partitioning of naphthenic acids in water–crude oil systems – determination through high-field NMR spectroscopy, Fuel 112: 236-248.

Moradi, S., Isari, A.A., Bachari, Z. and Mahmoodi, H., 2019. Combination of a new natural surfactant and smart water injection for enhanced oil recovery in carbonate rock: Synergic impacts of active ions and natural surfactant concentration. Journal of Petroleum Science and Engineering 176: 1-10.

Torrijos, I.D.P., Puntervold, T., Strand, S., Austad, T., Bleivik, T.H. and Abdullah, H.I., 2018. An experimental study of the low salinity Smart Water-polymer hybrid EOR effect in sandstone material. Journal of Petroleum Science and Engineering 164: 219-229.

Veiskarami, S., Jafari, A. and Soleymanzadeh, A., 2020. Phase behavior, wettability alteration, and oil recovery of low-salinity surfactant solutions in carbonate reservoirs. SPE Journal 25 (04): 1784-1802.

Verruto, V.J., Le, R.K., and Kilpatrick, P.K. 2009. Adsorption and molecular rearrangement of amphoteric species at oil–water interfaces. J Phys Chem B. 113 (42):13788–13799.

Wang, J., Han, M., Fuseni, A.B. and Cao, D. 2015. Surfactant adsorption in surfactant-polymer floodin in carbonate reservoirs. SPE 172700-MS. SPE Middle East Oil & Gas Show Conference. Manama, Bahrain.

Wang, J., Ayirala, S.C., AlSofi, A.M. and Yousef, A.A. 2018. SmartWater synergy with surfactant polymer flooding for efficient oil mobilization in carbonates. SPE EOR Conference at Oil and Gas West Asia, Muscat, Oman.

Yarranton, H.W., Urrutia, P. and Sztukowski, D.M. 2007. Effect of interfacial rheology on model emulsion coalescence. Journal of Colloid and Interface Science 310: 253-259.